Nanoscale Research Letters
a SpringerOpen Journal

NANO EXPRESS   **Open Access**

Adsorptive interaction of bisphenol A with mesoporous titanosilicate/reduced graphene oxide nanocomposite materials: FT-IR and Raman analyses

Chinh Nguyen-Huy[1], Nayoung Kim[1], Thuy-Duong Nguyen-Phan[2], Ik-Keun Yoo[1] and Eun Woo Shin[1*]

Abstract

Nanocomposite materials containing graphene oxide have attracted tremendous interest as catalysts and adsorbents for water purification. In this study, mesoporous titanosilicate/reduced graphene oxide composite materials with different Ti contents were employed as adsorbents for removing bisphenol A (BPA) from water systems. The adsorptive interaction between BPA and adsorption sites on the composite materials was investigated by Fourier transform infrared (FT-IR) and Raman spectroscopy. Adsorption capacities of BPA at equilibrium, q_e (mg/g), decreased with increasing Ti contents, proportional to the surface area of the composite materials. FT-IR observations for fresh and spent adsorbents indicated that BPA adsorbed onto the composite materials by the electrostatic interaction between OH functional groups contained in BPA and on the adsorbents. The electrostatic adsorption sites on the adsorbents were categorized into three hydroxyl groups: Si-OH, Ti-OH, and graphene-OH. In Raman spectra, the intensity ratios of D to G band were decreased after the adsorption of BPA, implying adsorptive interaction of benzene rings of BPA with the sp^2 hybrid structure of the reduced graphene oxide.

Keywords: Bisphenol A; Graphene oxide; Mesoporous titanosilicate; Adsorption sites; Interaction

Background

Endocrine-disrupting chemicals (EDCs) are substances that mimic natural hormones in the endocrine system causing adverse effects on humans and wildlife [1,2]. EDCs are considered to be exogenous agents that interfere with the synthesis, secretion, transport, binding, action, and elimination of natural hormones in the body responsible for the maintenance of homeostasis, reproduction, development, and behavior. Exposure to EDCs could have a substantial effect on the body, disrupting bodily functions and processes. Bisphenol A (BPA), an EDC, is a cause of considerable social and scientific concern. It is heavily used as a monomer in the synthesis of epoxy resins and polycarbonate plastics [3] and is considered to be a significant pollutant since its weak estrogen-like effect is harmful to organisms [3-5]. Various diseases (including carcinogenesis) may result from

exposure to BPA. In recent years, BPA has been detected in industrial wastewater, groundwater, surface water, and drinking water [6-9].

Various technologies have been attempted to remove BPA from water systems, such as adsorption [10-12], biological treatment [13], and photodegradation technology [14]. Among these methods, adsorption is a superior and promising method for removing low-concentration contaminants from water systems in terms of cost, ease of operation, and lack of harmful secondary products. The removal of pollutants by the adsorption process depends on the inherent physicochemical properties of the pollutants and adsorbents.

Graphene, a single sp^2-hybridized carbon layer arranged in a honeycomb structure, is currently one of the most exciting new materials due to its large surface area, excellent electronic and mechanical properties, and good thermal conductivity [15-17]. The remarkable properties of graphene allow it to be applied in many research fields, including adsorbents. Mesoporous silicate has been used for

* Correspondence: ewshin@ulsan.ac.kr
[1]School of Chemical Engineering, University of Ulsan, Daehakro 93, Nam-gu, Ulsan 680-749, South Korea
Full list of author information is available at the end of the article

Springer

environmental applications because of its large surface area and interconnected channels [18,19]. Ti has been incorporated into the framework of mesoporous silicate to significantly improve its hydrothermal stability, adsorbability, and photocatalytic performance [18-21]. Recently, the combination of graphene or reduced graphene oxide nanosheets and TiO_2 particles has been shown to be a promising candidate for both adsorption and photocatalysis in water systems owing to the improved accessibility to pollutants and efficient facilitation of charge carrier separation [22-25].

In this work, mesoporous titanosilicate/reduced graphene oxide composite materials were synthesized as a function of Ti content, and their adsorptive characteristic for BPA in an aqueous solution was investigated through FT-IR and Raman spectroscopy for the first time. FT-IR analysis showed that the hydroxyl groups on the composite materials interacted with BPA to produce hydrogen bonding and the hydroxyl groups in the mesoporous titanosilicate could be divided into two different types - Si-OH and Ti-OH. In addition, Raman spectra gave evidence that the sp^2 hybrid structure of graphene oxide interacted with the benzene rings of BPA. This work may provide new insights into adsorptive interactions between the adsorption sites of inorganic/organic composite materials and organic contaminants.

Methods

Preparation of composite materials

All chemicals were obtained from Sigma-Aldrich Korea (Yongin, Kyunggi, South Korea) and were used as received without any purification. In a typical procedure, graphene oxide (GO) was synthesized from expanded graphite (grade 1721, Asbury Carbons, Asbury, NJ, USA) by a modified Hummers method [26]. For the preparation of mesoporous titanosilicate/reduced graphene oxide composite materials, an aqueous solution containing cetyltrimethyl ammonium bromide (CTAB) and NaOH was mixed until it became homogeneous; then, the GO dispersion was added (approximately 10 wt%). The mixture was sonicated for 2 h at room temperature and then magnetically stirred at 313 K for 2 h. A mixture of tetraethyl orthosilicate and titanium isopropoxide (various Ti:Si molar ratios were used for different compositions) was added drop-wise. The whole solution was stirred at 313 K for 12 h and then hydrothermally treated at 353 K for 10 h. Solid products were recovered by washing with warm ethanol and drying at 353 K overnight. The as-synthesized powders were finally heat-treated at 823 K for 4 h under flowing Ar (15 ml/min). The calcined materials were denoted as '**MTSG-i**' for mesoporous titanosilicate/graphene composite materials, where 'i' is the Ti content (1, 5, 10, and 20 wt%).

Characterization techniques

Fourier transform infrared (FT-IR) spectra were obtained on a Nicolet 380 FT-IR spectrometer (Thermo Electron Co., Waltham, MA, USA) using the KBr pellet technique. Raman spectra were collected using a DRX Raman microscope (Thermo Fisher Scientific, Waltham, MA, USA) with a 633-nm laser excitation. N_2 sorption measurements were conducted on a Micromeritics ASAP 2020 instrument (Micromeritics, Norcross, GA, USA). The samples were degassed under a vacuum at 240°C for 5 h prior to automatic analyzer analysis at −196.15°C. The Brunauer-Emmett-Teller (BET) calculation method was applied to determine the specific surface area.

BPA adsorption

The adsorptivity of the composite materials was elucidated through the removal of BPA in water. Specifically, 50 mg of the adsorbent was immersed in 100 ml of the BPA-containing solution (initial concentration = 10 mg/l) under constant stirring inside a dark chamber. The pH of
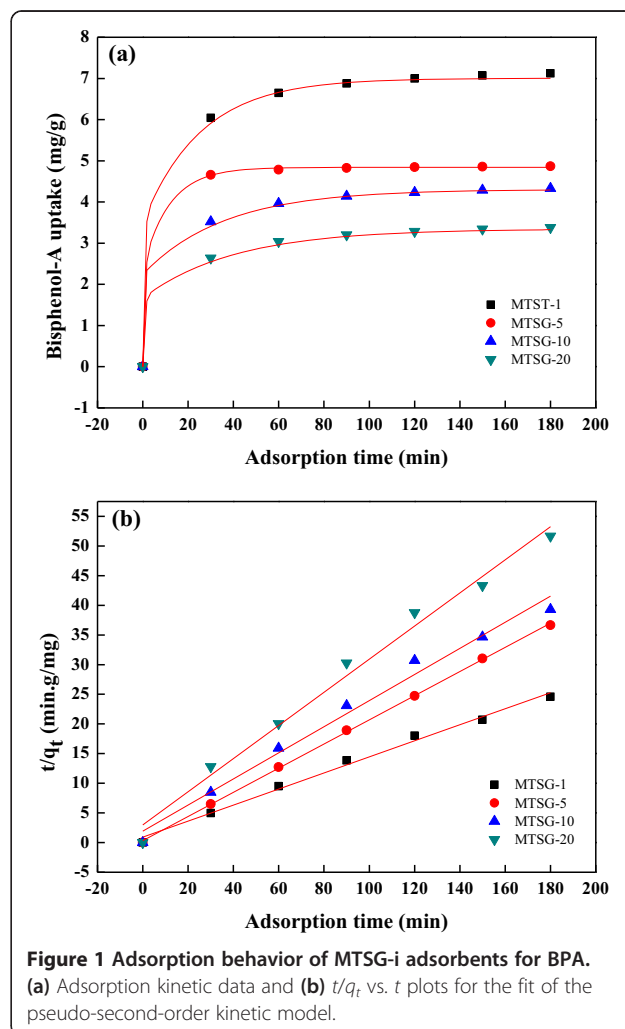
Figure 1 Adsorption behavior of MTSG-i adsorbents for BPA.
(a) Adsorption kinetic data and **(b)** t/q_t vs. t plots for the fit of the pseudo-second-order kinetic model.

Table 1 Adsorption amount at equilibrium (q_e) and coefficient of the pseudo-second-order model for BPA adsorption

Sample	Experimental $q_{e,exp}$ (mg/g$_{ads}$)[a]	Adsorption efficiency (%)[b]	k (g$_{ads}$/mg·min)[c]	q_e (mg/g$_{ads}$)[c]	R^2 value[c]	Surface area (m^2/g)[d]
MTSG-1	6.6488	36.6	0.0203	7.386	0.9934	891.3
MTSG-5	4.8821	24.6	0.1263	4.912	0.9996	804.5
MTSG-10	3.9987	22.9	0.0254	4.539	0.9863	737.8
MTSG-20	3.4748	17.4	0.0262	3.579	0.987	652.2

[a]Equilibrium adsorption capacity obtained from the kinetics experiment; [b]adsorption efficiency at the equilibrium state; [c]adsorption rate constant, equilibrium uptake, and correlation coefficient determined from the pseudo-second-order adsorption model (t/q_t vs. $f(t)$); [d]measured from N_2 adsorption/desorption.

the solutions was 6.0 ± 0.3. The concentration of the BPA solution before and after adsorption at room temperature was measured by a UV-vis absorbance microplate spectrophotometer (SpectraMax® Plus 384, Molecular Devices, Sunnyvale, CA, USA). The amount adsorbed onto the adsorbent, $q_{e,exp}$ (mg/g), was calculated by a mass balance relationship:

$$q_{e,exp} = (C_0 - C_e)\frac{V}{W} \qquad (1)$$

where C_0 and C_e are the initial and equilibrium liquid-phase concentrations of BPA (mg/l), V is the volume of the solution (l), and W is the weight of the dry composite materials used (g).

After adsorption tests, spent adsorbents were then filtered using a 0.22-μm GV filter, dried inside a hood, and wrapped in aluminum foil. Dried spent adsorbents were used for Raman and FT-IR analyses for observing the adsorption interaction between BPA and the adsorbents.

Results and discussion

Adsorption behavior

The adsorption behavior of MTSG-i for BPA was monitored by adsorption kinetics shown in Figure 1. With increasing Ti content, adsorption amounts at equilibrium (q_e) increased. To quantitatively measure the adsorption

behavior, a pseudo-second-order kinetic model was employed, resulting in q_e values and an adsorption rate constant (k_{ads}) from the fit of the adsorption kinetic data. Herein, the pseudo-second-order equation is in the form [27]:

$$\frac{dq_t}{dt} = k_{ads}(q_e - q_t)^2 \qquad (2)$$

Figure 3 FT-IR spectra of (a) fresh MTSG-i and (b) spent MTSG-i adsorbents.

Figure 2 A plot of adsorption amount at equilibrium (q_e) for BPA vs. surface area of MTSG-i adsorbents.
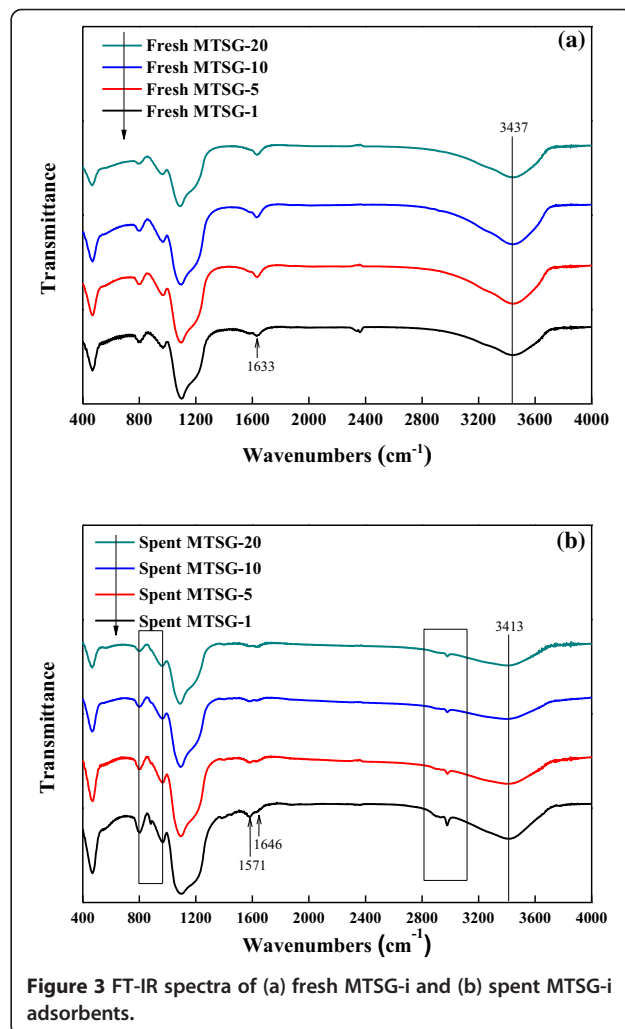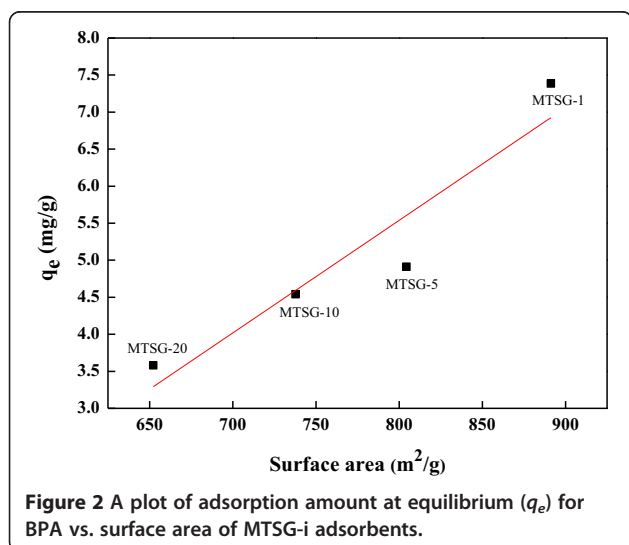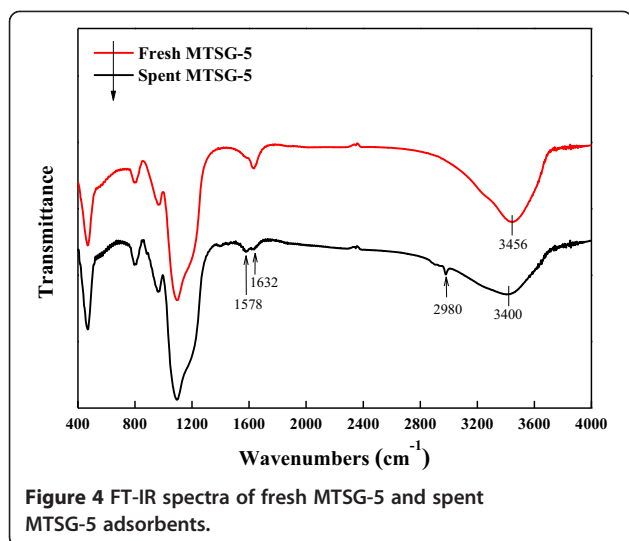
Figure 4 FT-IR spectra of fresh MTSG-5 and spent MTSG-5 adsorbents.
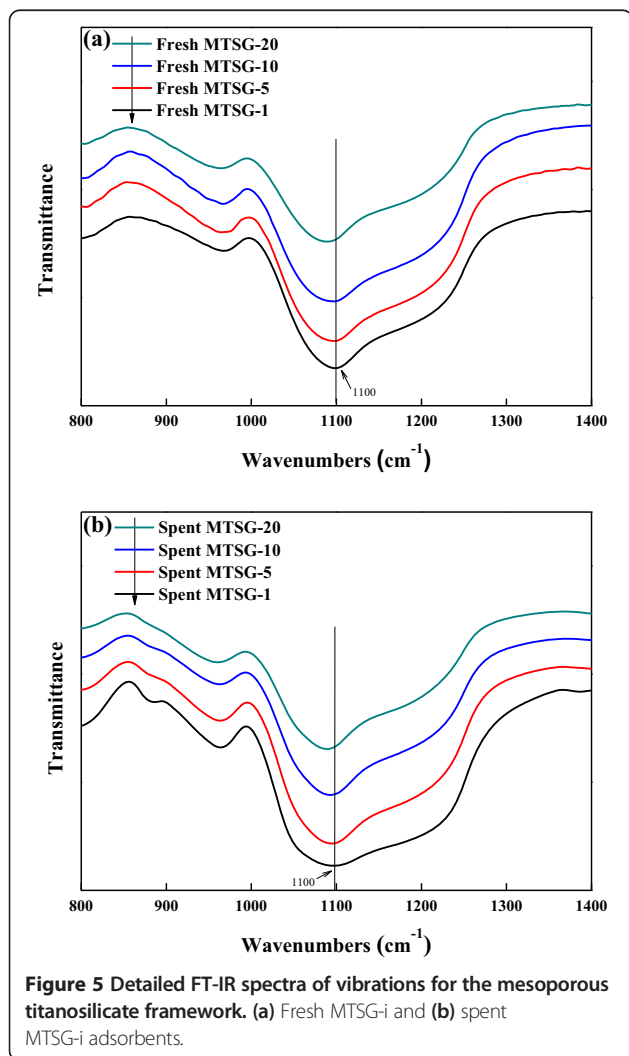
Figure 5 Detailed FT-IR spectra of vibrations for the mesoporous titanosilicate framework. (a) Fresh MTSG-i and **(b)** spent MTSG-i adsorbents.
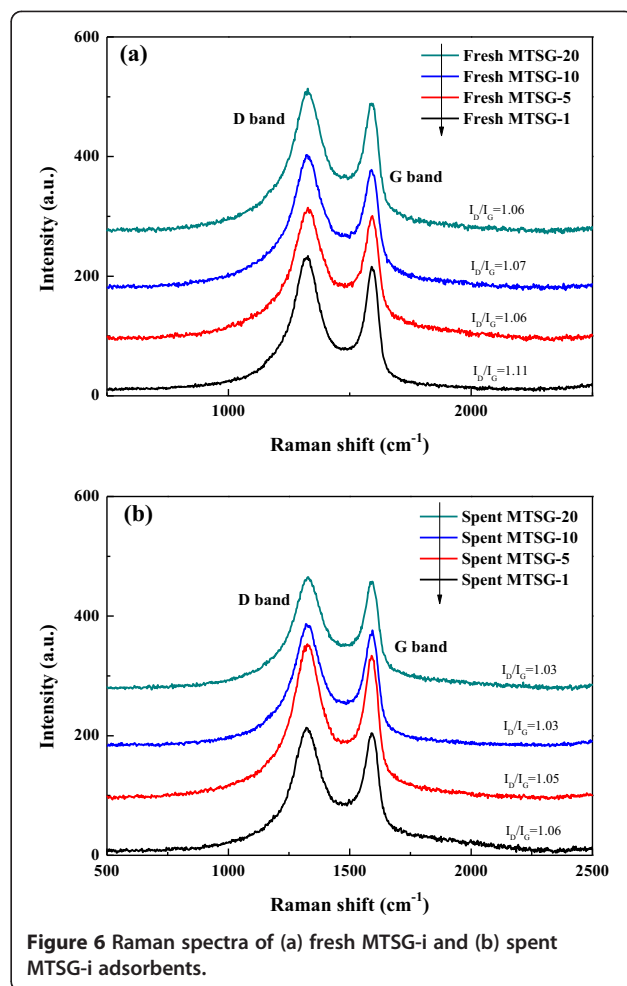
Figure 6 Raman spectra of (a) fresh MTSG-i and (b) spent MTSG-i adsorbents.

where q_e and q_t are the adsorption capacity at equilibrium and at time t, respectively (mg/g$_{catalyst}$) and k_{ads} is the rate constant of pseudo-second-order sorption (g$_{catalyst}$/mg · min). By integrating Equation 2 for the boundary conditions ($t = 0$ to $t = t$ and $q_t = 0$ to $q_t = q_t$), the following linear form can be written as:

$$\frac{t}{q_t} = \frac{1}{kq_e^2} + \frac{1}{q_e}t \qquad (3)$$

In the present study, the experimental data evaluated from the linear transform $(t/q_t) = f(t)$ conform to the pseudo-second-order adsorption kinetics. Therefore, the q_e and k_{ads} values are determined from the slope and intercept of the plot. The q_e and k_{ads} values obtained from the fits are listed in Table 1. Fitted q_e values are a little bit higher than the $q_{e,exp}$ values, but show the same trend for the Ti content, namely, that the values decrease with increasing Ti content. In the literature, Ti incorporation into the framework of mesoporous silicates enhanced hydrothermal stability, adsorbability, and photocatalytic performance [18,23]. However, it also induced

a decrease in surface area with increased Ti loading [19]. In this study, with the Ti incorporation, the surface areas of the composite materials decreased (Table 1). In Figure 2, the q_e values are plotted along with the surface area of the composite materials. It clearly shows that the q_e value is proportional to the surface area of the composite materials. Accordingly, the surface area of the composite materials is a key parameter for BPA adsorption, and the decrease in the q_e value of the composite materials is caused by a reduction in the surface area by Ti addition.

Adsorptive interaction of BPA with the composite materials

FT-IR spectra for fresh and spent adsorbents were collected to analyze the adsorptive interactions of BPA. Figure 3a,b shows FT-IR spectra of fresh and spent MTSG-i, respectively. Primary infrared bands related to the mesoporous titanosilicate framework are the asymmetric and symmetric stretch of Si-O-Si around 1,094 and 804 cm^{-1}, respectively. The band around 470 cm^{-1} is assigned to the Si-O bending vibration. Conventionally, the band around 962 cm^{-1} corresponds to the Si (or Ti)-OH vibration [28-31]. The broad bands around 3,400 to 3,450 cm^{-1} and 2,900 to 2,990 cm^{-1} represent OH and CH stretching modes, respectively. Assignment of the band at 1,634 cm^{-1} is important in this study. It can be assigned to the OH bending vibration of adsorbed water, the C = C skeleton vibration, or the C = O asymmetric stretching vibration. In this study, it should be assigned to the OH bending vibration since the intensity of the band closely correlates with that of the OH stretching vibration [28-31].

The change in FT-IR spectra after BPA adsorption is similar irrespective of the Ti content. Hence, to show the difference in FT-IR spectra by BPA adsorption in detail, FT-IR spectra of fresh and spent MTSG-5 are presented in Figure 4. The first change in FT-IR spectra as a result of BPA adsorption is the appearance of new IR bands around 2,900 to 2,990 cm^{-1} assigned to the CH stretching vibration. Those bands represent BPA adsorbed onto the composite materials. The second change in the FT-IR spectra is related to OH vibration. The band position of the OH stretching vibration is shifted from 3,448 to 3,400 cm^{-1}, and the band intensities of OH stretching (3,448 cm^{-1}) and bending (1,634 cm^{-1}) vibrations were decreased after BPA adsorption. These phenomena indicate that OH functional groups on the composite materials interacted with hydroxyl groups contained in BPA resulting in hydrogen bonding [32].

Meanwhile, there is a change in FT-IR spectra due to the Ti content. Figure 5 shows FT-IR spectra related to mesoporous titanosilicate. In Figure 5a, the band around
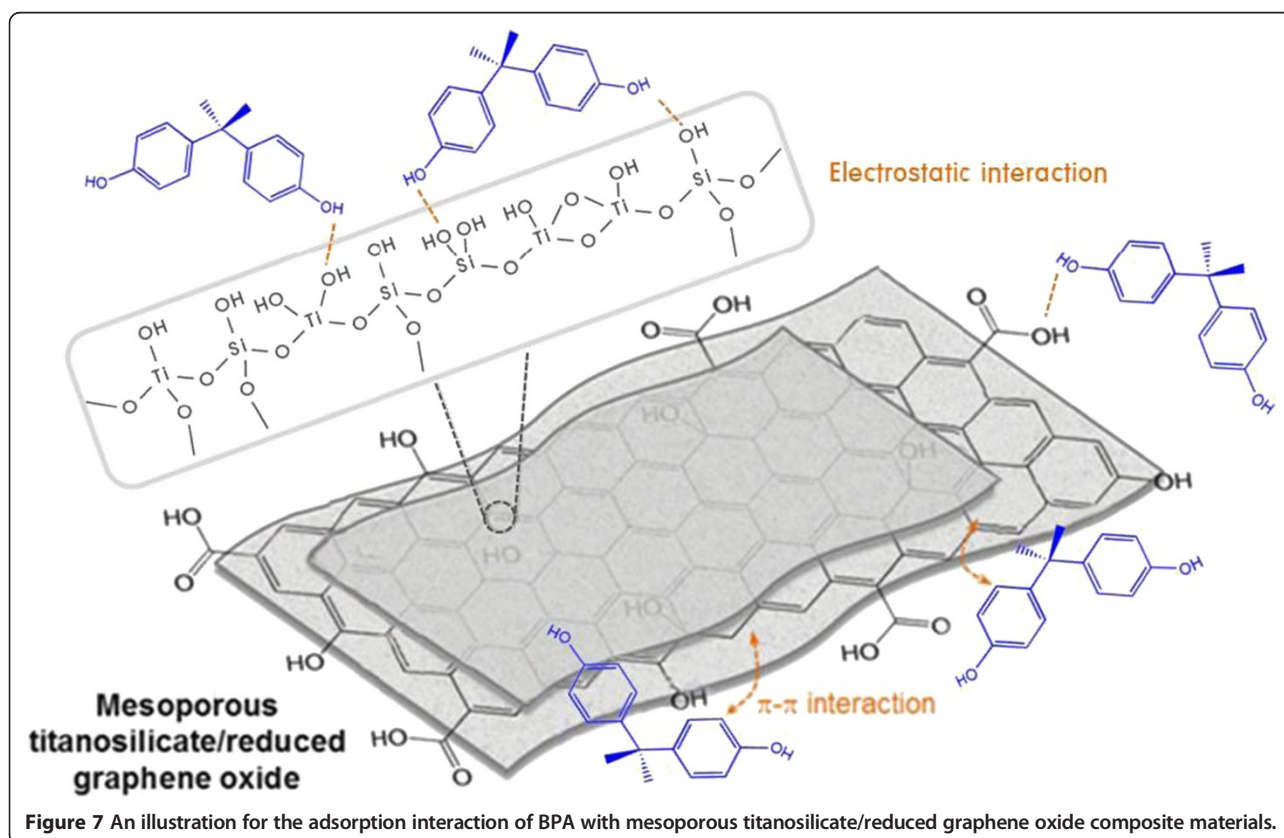
Figure 7 An illustration for the adsorption interaction of BPA with mesoporous titanosilicate/reduced graphene oxide composite materials.

1,090 cm^{-1}, representing the stretching mode of Si-O-Si, moves from 1,100 to 1,088 cm^{-1} with increasing Ti content. This is also observed even for spent MTSG-i. This implies that added Ti incorporates into the framework of mesoporous silicate to make Ti-O-Si or Ti-O-Ti bonds. Replacing Si atoms in the framework with Ti atoms induces a redshift in wave number because the wave number is inversely proportional to the root of the harmonic average of atomic mass. Consequently, based on the redshift of the band around 1,090 cm^{-1}, it can be concluded that there are at least two different types of hydroxyl groups even in the mesoporous titanosilicate structure: Si-OH and Ti-OH.

Raman spectra for fresh and spent MTSG-i were also collected to evaluate the adsorptive interaction between BPA and graphene oxide, shown in Figure 6. Two indicative D and G bands at 1,340 and 1,590 cm^{-1} of the composite materials are associated with the breakage of symmetry by edges or a high density of defects, and the first-order scattering of E$_{2g}$ vibration mode observed for the sp^2 domain, respectively [33]. The relative intensities of those broad bands for all MTSG-i decreased after BPA adsorption, illustrating either an increase in the average size of sp^2 domains or a change in the properties of the reduced graphene oxide sheets due to interactions with BPA. Accordingly, the decrease in I_D/I_G ratio by BPA adsorption implies the existence of π-π interactions between the benzene rings of BPA and the sp^2 domains of the reduced graphene oxide.

Figure 7 illustrates the adsorptive interaction of BPA with adsorption sites of mesoporous titanosilicate/reduced graphene oxide composite materials. BPA adsorbs onto mesoporous titanosilicate/reduced graphene oxide composite materials by either electrostatic interaction between the hydroxyl groups contained in BPA and the hydroxyl groups on the adsorbents or the π-π interaction between the benzene rings of BPA and the sp^2 domains of the reduced graphene oxide. In the case of the electrostatic interaction, the hydroxyl groups on the adsorbents can be divided into three different types of adsorbent sites, namely, OH on the reduced graphene oxide, OH bonded to Si atoms, and OH bonded to Ti atoms. However, it was observed that the adsorption amount was essentially proportional to the surface area of the composite materials.

Conclusions

We prepared mesoporous titanosilicate/reduced graphene oxide composite materials with different Ti contents and used them as adsorbents for removing BPA from a water system. Adsorption amounts acquired from adsorption kinetics are inversely proportional to the Ti content since the surface areas of the composite materials decreased with increasing Ti content. In this study, the adsorptive interaction of BPA with the adsorbents was observed by FT-IR and Raman analyses. From the observation, we reached the conclusion that BPA is adsorbed onto the composite materials through two different interactions: (i) electrostatic interactions between the hydroxyl groups of BPA and mesoporous titanosilicate or reduced graphene oxide and (ii) π-π interactions between the benzene rings of BPA and the sp^2 domains of reduced graphene oxide.

Authors' contributions
NK performed the adsorption tests and drew the figures. CNH characterized the samples with Raman and FT-IR. TDNP designed the experiments and synthesized the samples. IKY was involved in the writing process. EWS designed the experiments and wrote the manuscript. All authors have read and approved the final manuscript.

Author details
[1]School of Chemical Engineering, University of Ulsan, Daehakro 93, Nam-gu, Ulsan 680-749, South Korea. [2]Chemistry Department, Brookhaven National Laboratory, Upton, New York 11973, USA.

References
1. Temes TA, Stumpf M, Mueller J, Haberer K, Wilken RD, Servos M: **Behavior and occurrence of estrogens in municipal sewage treatment plants—I. Investigations in Germany, Canada and Brazil.** *Sci Total Environ* 1999, **225**:81–90.
2. Chang HS, Choo KH, Lee B, Choi SJ: **The methods of identification, analysis, and removal of endocrine disrupting compounds (EDCs) in water.** *J Hazard Mater* 2009, **172**:1–12.
3. Staples CA, Dome PB, Klecka GM, Oblock ST, Harris LR: **A review of the environmental fate, effects, and exposures of bisphenol A.** *Chemosphere* 1998, **36**:2149–2173.
4. Furhacker M, Scharf S, Weber H: **Bisphenol A: emissions from point sources.** *Chemosphere* 2000, **41**:751–756.
5. Kang JH, Kondo F, Katayama Y: **Human exposure to bisphenol A.** *Toxicol* 2006, **226**:79–89.
6. Kolpin DW, Furlong ET, Meyer MT, Thurman EM, Zaugg SD, Barber LB, Buxton HT: **Pharmaceuticals, hormones, and other organic wastewater contaminants in US streams, 1999–2000: a national reconnaissance.** *Environ Sci Technol* 2002, **36**:1202–1211.
7. Yamamoto T, Yasuhara A, Shiraishi H, Nakasugi O: **Bisphenol A in hazardous waste landfill leachates.** *Chemosphere* 2001, **42**:415–418.
8. Belfroid A, van Velzen M, van der Horst B, Vethaak D: **Occurrence of bisphenol A in surface water and uptake in fish: evaluation of field measurements.** *Chemosphere* 2002, **49**:97–103.
9. Flint S, Markle T, Thompson S, Wallace E: **Bisphenol A exposure, effects, and policy: a wildlife perspective.** *J Environ Manage* 2012, **104**:19–34.
10. Liu G, Ma J, Li X, Qin Q: **Adsorption of bisphenol A from aqueous solution onto activated carbons with different modification treatments.** *J Hazard Mater* 2009, **164**:1275–1280.
11. Dong Y, Wu D, Chen X, Lin Y: **Adsorption of bisphenol A from water by surfactant-modified zeolite.** *J Colloid Interf Sci* 2010, **348**:585–590.
12. Tsai W, Hsu H, Su T, Lin K, Lin C: **Adsorption characteristics of bisphenol-A in aqueous solutions onto hydrophobic zeolite.** *J Colloid Interf Sci* 2006, **299**:513–519.

13. Gomez M, Garralon G, Plaza F, Vilchez R, Hontoria E, Gomez MA: **Rejection of endocrine disrupting compounds (bisphenol A, bisphenol F and triethyleneglycol dimethacrylate) by membrane technologies.** *Desalination* 2007, **212**:79–91.

14. Belgiorno V, Rizzo L, Fatta D, Della Rocca C, Lofrano G, Nikolaou A, Naddeo V, Meric S: **Review on endocrine disrupting-emerging compounds in urban wastewater: occurrence and removal by photocatalysis and ultrasonic irradiation for wastewater reuse.** *Desalination* 2007, **215**:166–176.

15. Meyer JC, Geim AK, Katsnelson MI, Novoselov KS, Booth TJ, Roth S: **The structure of suspended graphene sheets.** *Nature* 2007, **446**:60–63.

16. Lee C, Wei X, Kysar JW, Hone J: **Measurement of the elastic properties and intrinsic strength of monolayer graphene.** *Science* 2008, **321**:385–388.

17. Balandin AA, Ghosh S, Bao W, Calizo I, Teweldebrhan D, Miao F, Lau CN: **Superior thermal conductivity of single-layer graphene.** *Nano Lett* 2008, **8**:902–907.

18. Carreon MA, Guliants VV: **Ordered meso and macroporous binary and mixed metal oxides.** *Eur J Inorg Chem* 2005, **1**:27–43.

19. Sinha AK, Seelan S, Okumura M, Akita T, Tsubota S, Haruta M: **Three-dimensional mesoporous titanosilicates prepared by modified sol-gel method: ideal gold catalyst supports for enhanced propene epoxidation.** *J Phys Chem B* 2005, **109**:3956–3965.

20. Chen X, Mao SS: **Titanium dioxide nanomaterials: synthesis, properties, modifications, and applications.** *Chem Rev* 2007, **107**:2891–2959.

21. Messina PV, Schulz PC: **Adsorption of reactive dyes on titania-silica mesoporous materials.** *J Colloid Interface Sci* 2006, **299**:305–320.

22. Nguyen-Phan TD, Pham VH, Shin EW, Pham HD, Kim S, Kim EJ, Chung JS, Hur SH: **The role of graphene oxide content on the adsorption-enhanced photocatalysis of titanium dioxide/graphene oxide composites.** *Chem Eng J* 2011, **170**:226–232.

23. Nguyen-Phan TD, Shin EW, Pham VH, Kweon H, Kim S, Kim EJ, Chung JS: **Mesoporous titanosilicate/reduced graphene oxide composites: layered structure, high surface-to-volume ratio, doping effect and application in dye removal from water.** *J Mater Chem* 2012, **22**:20504–20511.

24. Leary R, Westwood A: **Carbonaceous nanomaterials for the enhancement of TiO$_2$ photocatalysis.** *Carbon* 2011, **49**:741–772.

25. Ramesha GK, Kumara V, Muralidhara HB, Sampath S: **Graphene and graphene oxide as effective adsorbents toward anionic and cationic dyes.** *J Colloid Interface Sci* 2011, **361**:270–277.

26. Hummers WS, Offeman RE: **Preparation of graphitic oxide.** *J Am Chem Soc* 1958, **80**:1339–1339.

27. Ho YS, McKay G: **A comparison of chemisorption kinetic models applied to pollutant removal on various sorbents.** *Trans Inst Chem Eng* 1988, **76B**:332–340.

28. Calabro DC, Valyoscik EW, Ryan FX: **In situ ATR/FTIR study of mesoporous silicate syntheses.** *Micropor Meter* 1996, **7**:243–259.

29. Hamid S, Syed W-H, Mohammad G-M: **Synthesis and characterization of amino-functionalized mesoporous silicate MCM-41 for removal of toxic metal ions.** *Chin J Chem* 2009, **27**:915–919.

30. Garcia R, Diaz I, Marquez-Alvarez C, Perez-Pariente J: **An approach toward the synthesis of platelike ordered mesoporous materials from layered zeolite precursors.** *Chem Mater* 2006, **18**:2283–2292.

31. Li Z, Gao L, Zheng S: **SEM, XPS, and FTIR studies of MoO$_3$ dispersion on mesoporous silicate MCM-41 by calcinations.** *Mater Lett* 2003, **57**:4605–4610.

32. Xu J, Wang L, Zhu Y: **Decontamination of bisphenol A from aqueous solution graphene adsorption.** *Langmuir* 2012, **28**:8418–8425.

33. Tuinstra F, Koenig JL: **Raman spectrum of graphite.** *J Chem Phys* 1970, **53**:1126–1130.